

Title: Reference dimensions to determine valve size of stented surgical aortic bioprostheses by computed tomography.

Authors: Malcom Anastasius, MBBS, MM, PhD; Marcelo Godoy, M.D; Jonathan R. Weir-McCall, MBChB, PhD; Vinayak Bapat, M.D; Janarthanan Sathananthan, MBChB, MPH; Mark Hensey, MB, BCH, BAO; Stephanie L. Sellers, PhD; Anson Cheung, M.D; Jian Ye, M.D; David A Wood, M.D; Jonathon Leipsic, M.D, FSCCT; John Webb, M.D; Philipp Blanke, M.D ,FSCCT

DOI: 10.4244/EIJ-D-19-00921

Citation: Anastasius M, Godoy M, Weir-McCall JR, Bapat V, Sathananthan J, Hensey M, Sellers SL, Cheung A, Ye J, Wood DA, Leipsic J, Webb J, Blanke P. Reference dimensions to determine valve size of stented surgical aortic bioprostheses by computed tomography. *EuroIntervention* 2020; Jaa-722 2020, doi: 10.4244/EIJ-D-19-00921

Manuscript submission date: 08 October 2019

Revisions received: 15 January 2020, 26 January 2020

Accepted date: 30 January 2020

Online publication date: 04 February 2020

Disclaimer: This is a PDF file of a "Just accepted article". This PDF has been published online early without copy editing/typesetting as a service to the Journal's readership (having early access to this data). Copy editing/typesetting will commence shortly. Unforeseen errors may arise during the proofing process and as such Europa Digital & Publishing exercise their legal rights concerning these potential circumstances.

Reference dimensions to determine valve size of stented surgical aortic bioprostheses by computed tomography

Malcom Anastasius¹ MBBS MM PhD, Marcelo Godoy¹ MD, Jonathan R. Weir-McCall² MBChB PhD, Vinayak Bapat³ MD, Janarthanan Sathanathan¹ MBChB, MPH, Mark Hensey¹ MB, BCH, BAO, Stephanie L. Sellers⁴ PhD, Anson Cheung¹ MD, Jian Ye¹ MD, David A Wood¹ MD, Jonathon Leipsic¹ MD FSCCT, John Webb¹ MD, Philipp Blanke¹ MD FSCCT

¹ Center for Heart Valve Innovation, St Paul's Hospital and University of British Columbia, Vancouver, BC, Canada

² Department of Radiology, University of Cambridge, Papworth Hospital, Cambridge, United Kingdom

³ Division of Cardiology, New York-Presbyterian Hospital, Columbia University Medical Center, New York, NY, USA.

⁴ Centre for Heart Lung Innovation and Department of Radiology, University of British Columbia & St. Paul's Hospital, Vancouver, BC, Canada

Short Title: SHV Sizing by CT

Address for Correspondence:

Philipp Blanke, MD, FSCCT
Assistant Professor, University of British Columbia
Department of Radiology, St. Paul's Hospital
1081 Burrard St.,
Vancouver, British Columbia, Canada V6Z 1Y6
Ph: 604-806-8026
Fax: 604-806-8283
phil.blanke@gmail.com

Financial disclosures

Dr. Leipsic serves as a consultant and has stock options in HeartFlow and Circle Cardiovascular Imaging, and receives speaking fees from GE Healthcare. Dr. Webb is a consultant to, and has received research funding from, Edwards Lifesciences,

Disclaimer : As a public service to our readership, this article -- peer reviewed by the Editors of EuroIntervention - has been published immediately upon acceptance as it was received. The content of this article is the sole responsibility of the authors, and not that of the journal

Abbott Vascular, and ViVitro Labs. Dr Wood is a consultant to Edwards Lifesciences and receives grant support from Edwards Lifesciences, Abbott Vascular, AstraZenca and Boston Scientific. Dr Sathananthan has received speaking fees and is a consultant to Edwards Lifesciences. Dr. Blanke is a consultant for Edwards Lifesciences and Circle Cardiovascular Imaging; and provides CT core lab services for Edwards Lifesciences, Medtronic, Neovasc, and Tendyne Holdings, for which he receives no direct compensation. All other authors have reported that they have no relationships relevant to the contents of this paper to disclose.

Keywords: Valve-in-valve, MSCT, Non-invasive imaging

Abbreviations:

aVIV: aortic valve-in-valve procedure

CT: Computed tomography

SHV: Bioprosthetic (stented) surgical heart valve

THV: Transcatheter heart valve

Acknowledgements: The authors wish to acknowledge the support provided by Drs Bruce McManus and Paul Hanson in the Cardiovascular Tissue Registry at St. Paul's Hospital

Introduction

Aortic valve-in-valve (aVIV) procedures are advancing the management of failed bioprosthetic surgical heart valves (SHV) (1,2). As opposed to transcatheter heart valve (THV) replacement for native aortic stenosis, selection of the transcatheter THV size for aVIV procedures is based on the SHV size and not on anatomical measurements. However, accurate SHV size information may not be available in medical records. While computed tomography (CT) may be used to derive dimensions of the SHV, it does have limitations (see later) (3). The aim of this study was to establish reference data for CT dimensions across commonly used aortic stented SHV types and sizes in order to determine the manufacturer's labeled size from a CT dataset.

Material & Methods

Study population. CT datasets of patients who underwent aVIV planning for failed SHV at St. Paul's Hospital (Vancouver, BC) between 2013 and 2018 were included. We also obtained 25 specimens from the Cardiovascular Tissue Registry at the Centre for Heart Lung Innovation (University of British Columbia & St. Paul's Hospital), to provide a more complete representation of commonly encountered SHVs (*ex vivo* imaging). Manufacturer labeled SHV size was determined from medical records. The Research Ethics Board, at the University of British Columbia – Providence Health Care approved this study

See supplement for CT data acquisition and reconstruction, CT image and statistical analysis.

CT image analysis was performed as follows: first, the reconstruction phase with the best image quality was identified. Using multiplane reformats, a plane transecting through the basal ring was created. Measurements were performed by fitting a circular region of interest to the center of the radiopaque scaffold, to yield area and diameter.

Results

Average patient age at the time of CT imaging was 72 ± 13 years. 101 (69%) were male. Median time between the initial SHV implantation and time of CT was 9.0 years (Interquartile range 4 years).

Derivation of the study cohort is shown in Figure 1. CT appearance and alignment of the region for interest for measurement of SHV size are illustrated in Figure 2, for 10 common valve types. Measurement results are listed in Table 1 and illustrated in Figure 2&3. There was excellent correlation between the CT-derived SHV size and the manufacturer size for all SHVs (Supplementary Figure 1,2 & 3).

Discussion

There is increasing adoption of aVIV procedures for patients with failed surgical aortic bioprosthetic valves, given growing evidence that the procedure is safe and effective (1,2). In planning for an aVIV procedure, CT may be used for measurement of the SHV size.

For planning an aVIV procedure, existing SHV size information is essential for determining THV size (4). Lack of SHV sizes in aVIV procedures can lead to incorrect THV size selection, resulting in either undersizing and paravalvular leak or device embolization, or oversizing leading to incomplete THV expansion and high transprosthetic gradients (1). Patient SHV size documentation may be absent and thus determining SHV size from CT seems desirable, with CT imaging already required for aVIV planning (5).

CT-based *in vivo* SHV sizing data is limited to a single study that evaluated SHVs by measuring the inner contour of the basal sewing ring (6). Importantly, the present study provides a more complete collection of valve types and sizes, and the measurement technique allows for more robust translation to CT systems with different acquisition and reconstruction settings. We deliberately assessed CT dimensions along the center of the radiopaque basal frame, to reduce the impact of acquisition and reconstruction technique as well as artifacts.

CT-based SHV dimension assessment can be affected by artifacts due to the radiopaque component of the basal frame and sewing ring. These artifacts include, blooming artifacts due to partial volume averaging as well as beam-hardening and streak artifacts. Blooming artifacts lead to overestimation of the metal component size, and thus to an underestimation when attempting to derive an internal diameter of the SHV from CT. Similarly, streak artifacts can impair accurate contour detection. Further, the extent of blooming and streak artifacts are influenced by tube potential, reconstruction technique and kernel, and window settings, as explained in the supplement (7). Given these factors influence the appearance of metal components', assessment of an internal diameter appears less robust. Instead, the technique employed in this study is independent of the above factors, by measuring along the center of the visualized radiopaque basal frame.

Measurement variability within individual valve type and size was limited. Only the Mitroflow SHV demonstrated higher measurement variability, due to the non-planar configuration of the basal ring. There was no overlap among assessed dimensions between different labeled valve sizes, permitting unambiguous determination of the labeled SHV size.

There is systematic discrepancy between the stent ID, defined as the inner diameter of the stent frame when covered with fabric or pericardium but without the valve leaflets and the true ID, accounting for the valve leaflet insertions (4). Importantly, CT does not appear capable of assessing the stent ID given the abovementioned impact on assessing the inner frame contour, nor can CT assess the true ID, which can only be assessed on a bench top. Thus, in the authors' opinion, CT assessment should include a reproducible SHV size measurement, with subsequent comparison to a reference chart

for determining the manufacture's labeled valve size, which can then be used to ascertain the stent ID and true ID, and the appropriate THV size using existing resources (8).

Study limitations

This is a single center study, with the available valve types and sizes limited to local practice. Older generation SHVs not commonly encountered in current clinical practice, such as the Carpentier-Edwards Standard were not included (9). The mechanism of aortic SHV degeneration and presence of pannus were not taken into account in the CT measurement.

Conclusion

The study provides a comprehensive reference chart of CT-derived SHV dimensions to allow identification of the manufacturers' labeled size from CT measurements, and facilitate THV sizing for aVIV procedures.

Impact on Daily practice

CT may be used to determine the manufacturer labeled SHV size and guide aVIV procedural planning.

Funding: None

References

1. Dvir D, Webb J, Brecker S, Bleiziffer S, Hildick-Smith D, Colombo A, Descoutures F, Hengstenberg C, Moat N, Bekerredjian R, Napodano M, Testa L, Lefevre T, Guetta V, Nissen H, Hernandez J, Roy D, Teles R, Segev A, Dumonteil N, Fiorina C, Gotzmann M, Tchetché D, Abdel-Wahab M, De Marco F, Baumbach A, Laborde J, Kornowski R. Transcatheter Aortic Valve Replacement for Degenerative Bioprosthetic Surgical Valves. Results From the Global Valve-in-Valve Registry. *Circulation* 2012;126:2335-2344.
2. Tuzcu E, Kapadia S, Vemulapalli S, Carroll J, Holmes D, Mack M, Thourani V, Grover F, Brennan J, Suri R, Dai D, Svensson L. Transcatheter Aortic Valve Replacement of Failed Surgically Implanted Bioprostheses. *Journal of the American College of Cardiology* 2018;72:370-82.
3. Rajani R, Attia R, Condemi F, Webb J, Woodburn P, Hodson D, Nair A, Preston R, Razavi R, Bapat V. Multidetector computed tomography sizing of bioprosthetic valves: guidelines for measurement and implications for valve-in-valve therapies. *Clinical Radiology* 2016;71:e41-e48.
4. Bapat V, Attia R, Thomas M. Effect of Valve Design on the Stent Internal Diameter of a Bioprosthetic Valve. A Concept of True Internal Diameter and Its Implications for the Valve-in-Valve Procedure. *JACC: Cardiovascular interventions* 2014;7:115-27.
5. Blanke P, Weir-McCall J, Achenbach S, Delgado V, Hausleiter J, Jilaihawi H, Marwan M, Norgaard B, Piazza N, Schoenhagen P, Leipsic J. Computed tomography imaging in the context of transcatheter aortic valve implantation (TAVI) / transcatheter aortic valve replacement (TAVR): An expert consensus

- document of the Society of Cardiovascular Computed Tomography. Journal of Cardiovascular Computed Tomography 2019;13:1-20.
6. Sucha D, Symersky P, Tanis W, Mali W, Leiner T, van Herwerden L, Buddle R. Multimodality Imaging Assessment of Prosthetic Heart Valves. Circulation Cardiovascular Imaging 2015;8:e003703.
 7. Kalisz K, Buethe F, Saboo S, Abbara S, Halliburton S, Rajiah P. Artifacts at Cardiac CT: Physics and Solutions. Radiographics 2016;36:2064-2083.
 8. Bapat V. Valve-in-valve apps: why and how they were developed and how to use them. Eurointervention 2014;10:U44-U51.
 9. Jamieson W, Burr L, Junsz M, Munro A, Hayden R, Miyagishima R, Ling H, Fradet G, Lichtenstein S, Stewart K. Carpentier-Edwards Standard and Supraannular Porcine Bioprostheses: Comparison of Technology. Annals of Thoracic Surgery 1999;67:10-17.

Legends

Figure 1 - Flow diagram demonstrating patient inclusion and exclusion.

Figure 2 - Lateral and en face CT volume-rendered images and multiplanar reformats aligned with the basal SHV ring, demonstrating circular ROI measurement (red circle) centered within the radiopaque contour (bone window) for 10 commonly used SHVs.

Figure 3 - (Figure 2 continued as Figure 3) Mosaic and Epic: measurement performed by fitting a circular ROI to the center of the thin radiolucent sewing ring

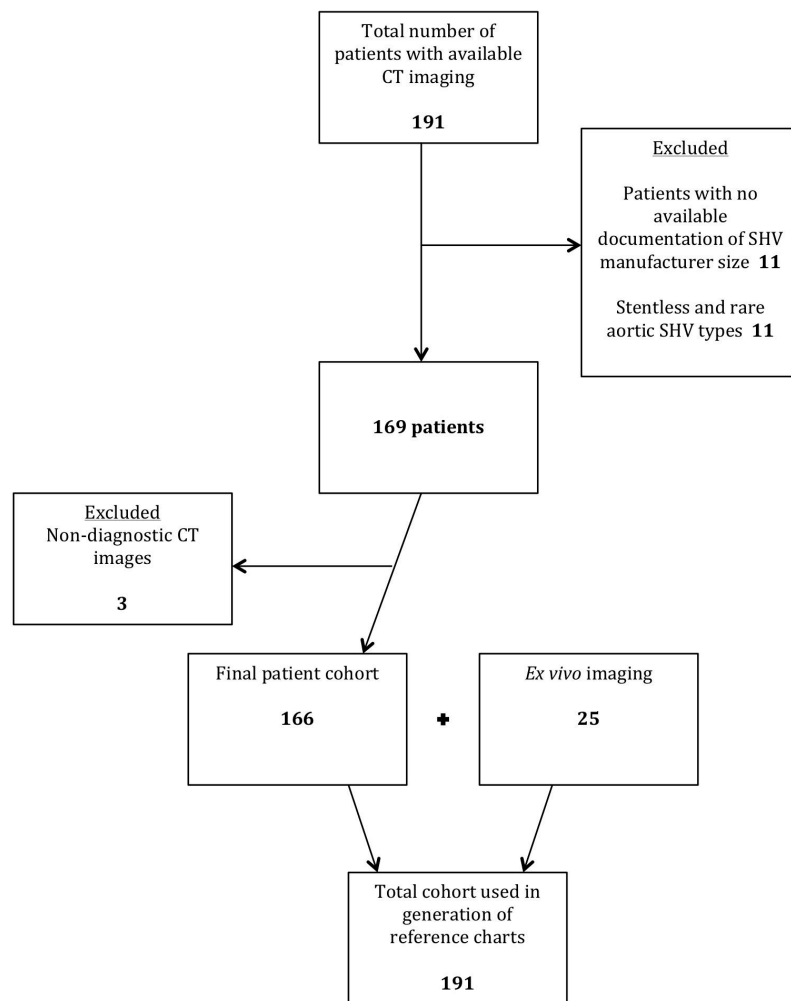
Table 1 – Reference chart of CT-derived SHV dimensions and manufacturers' labeled size

Aortic SHV	Manufacturer ID (mm)	CT Diameter (mm)	CT area (mm ²)	n
Perimount Magna Ease (Model 3300TFX)	19	Data n/a		
	21	20.4 ± 0.4	327 ± 10	5
	23	22.7 ± 0.4	407 ± 13	2
	25	24.5 ± 0.5	472 ± 17	10
	27	26.8 ± 0.1	568 ± 6	5
	29	28.9 ± 0.2	610 ± 110	5
Perimount Magna (Model 3000TFX)	19	Data n/a		
	21	20.7 ± 0.2	353 ± 46	7
	23	22.6 ± 0.3	401 ± 8	9
	25	24.8 ± 0.3	483 ± 10	8
	27	26.8 ± 0.3	570 ± 13	8
	29	29.1 ± 0.1	670 ± 11	2
Perimount (Model 2900)	19	Data n/a		
	21	20.8 ± 0.5	341 ± 12	6
	23	22.6 ± 0.2	401 ± 8	2
	25	24.6 ± 0.3	476 ± 138	6
	27	26.9 ± 0.1	563 ± 20	2
	29	n/a		
Carpentier-Edwards Supra-annular valve	19	n/a		
	21	21.1 ± 0.2	350 ± 5	3
	23	23.1 ± 0.2	419 ± 6	5
	25	25.0 ± 0.2	492 ± 6	3
	27	27.1 ± 0.2	578 ± 7	4
	29	n/a		
Perimount (Model 2700)	19	n/a		
	21	20.7 ± 0.2	340 ± 5	5
	23	22.7 ± 0.1	408 ± 5	7
	25	25.1	496 ± 2	1
	27	26.6 ± 0.1	558 ± 10	2
	29	n/a		
Mosaic (Model 305)	19	n/a		
	21	21.1	349	1
	23	22.7 ± 0.1	406 ± 5	5
	25	24.7 ± 0.2	482 ± 10	8
	27	26.9 ± 0.2	570 ± 7	6
	29	28.8 ± 0.1	656 ± 2	3

Mitroflow	19	n/a		
	21	21.5 ± 0.3	361 ± 7	6
	23	23.4 ± 0.3	431 ± 12	15
	25	25.5 ± 0.5	452 ± 7	8
	27	27.4 ± 0.02	596 ± 2	2
	29	n/a		
Trifecta	19	n/a		
	21	20.5 ± 0.04	333 ± 2	7
	23	22.5 ± 0.05	386 ± 32	4
	25	24.6 ± 0.1	477 ± 5	2
	27	26.6 ± 0.0	559 ± 2	2
	29	28.5	642	1
Epic	19	n/a		
	21	21.1	350 ± 3	2
	23	22.7	404.0	1
	25	25.2 ± 0.1	498 ± 0	2
	27	26.8 ± 0.1	559 ± 3	2
	29	28.4	638.0	1
Hancock	19	n/a		
	21	n/a		
	23	22.8 ± 0.5	408 ± 19	5
	25	25.1 ± 0.1	496 ± 3	2
	27	26.9	571	1
	29	29.2 ± 0.2	672 ± 8	2


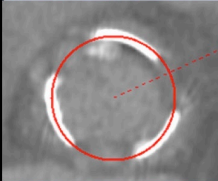
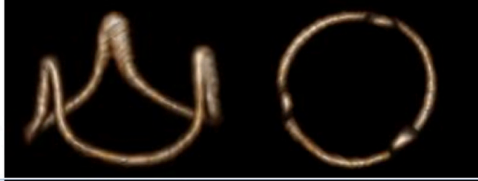
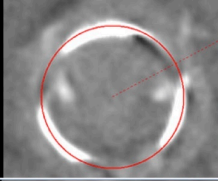

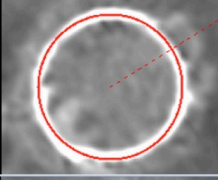

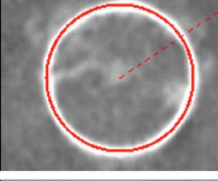

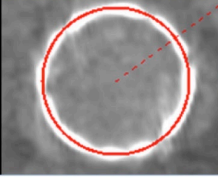
CT area and diameter stratified by manufacturer labeled SHV size; data are presented as mean ± SD; n, number of valves studied. ID: internal diameter, n/a: data not available

Figure 1 – Flow chart illustrating derivation of study cohort

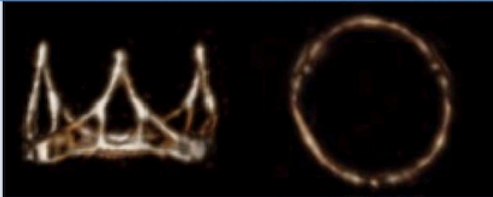
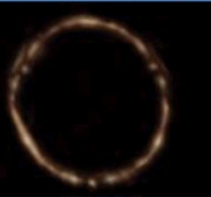










COR

Figure 2 – CT appearance and measurement technique

Valve	Volume rendered reconstructions & Measurement technique		CT appearance
Carpentier-Edwards Supra-Annular Valve (SAV) (Edwards Lifesciences)			Radiopaque elgiloy metal wire stent, three posts and a discontinuous base. One wire connection at one base. Transition from valley to post smoother than in CE Standard.
Perimount 2700 (Edwards Lifesciences)			Radiopaque cobalt-chromium frame, three posts and a discontinuous base. One wire connection at one post apparent as asymmetric thickening of a single post.
Perimount (Model 2900) (Edwards Lifesciences)			Radio-opaque undulating basal ring. Continuous thin stent frame above the base forming three radio-opaque posts.
Perimount Magna (Model 3000TFX) (Edwards Lifesciences)			Radiopaque undulating basal ring with regular indentations. Continuous thin stent frame above the base forming three radio-opaque posts.
Perimount Magna Ease (Model 3300TFX) (Edwards Lifesciences)			Radiopaque undulating basal ring with single indentation at peak. Continuous thin stent frame above the base forming three radio-opaque posts.

Copyright

Valve	Volume rendered reconstructions & Measurement technique		CT appearance
Trifecta (St. Jude Medical)			Radiopaque titanium stent frame forming a three-pronged coronet with undulating base.
Hancock II (Medtronic)			Floating radiopaque markers at the top of radiolucent stent posts. Undulating radiopaque sewing ring.
Mosaic (Model 305) (Medtronic)			Floating radiopaque markers at the peak of radiolucent stent posts. Radiolucent sewing ring.
Mitroflow (Sorin)			Undulating radiopaque sewing ring, radiolucent stent posts.
Epic (St. Jude Medical)			Thin radiopaque sewing ring with one focal area which appears thicker (wire connector); radiolucent stent posts.

Copyright

Supplementary material

Supplement - Methods

Study population. CT data sets of patients who underwent planning for a potential aVIV procedure for failed SHV at St. Paul's Hospital (Vancouver, BC) between October 2013 and December 2018 were included (*in vivo* imaging). We also obtained 25 specimens from the Cardiovascular Tissue Registry at the Centre for Heart Lung innovation (University of British Columbia & St. Paul's Hospital), to provide a more complete representation of commonly encountered SHVs (*ex vivo* imaging). The Research Ethics Board, at the University of British Columbia – Providence Health Care approved this study. Medical records for all patients were reviewed to determine SHV type and manufacturer labeled SHV size recorded at the time of original surgical bioprosthetic valve replacement. Only patients with stented valves were included.

Patients with an unknown valve type or size, rare valve types that did not sufficiently cover the current employed valve sizes, or incomplete documentation, were excluded from this analysis. Patients with stentless valves were excluded, given the absence of radiopaque structures for CT measurement as well as variable configuration due to the lack of a rigid scaffold (Figure 1).

CT data acquisition and reconstruction. CT images of surgical heart valves were acquired using either a wide detector CT scanner (GE Revolution or GE 750HD, General Electric, Milwaukee). CT images were acquired and reconstructed according to current guidelines (5), employing retrospective ECG-gating, thin sliced collimation of 0.625mm, 120 kVP tube voltage and tube current adjusted to body habitus. Images

were reconstructed as multiphase datasets in 10% intervals using a soft-tissue convolution kernel. *Ex vivo* specimens were scanned using similar acquisition and reconstruction parameters, without ECG-gating.

Contrast enhanced CT-images, obtained as part of recommended routine planning of aVIV procedures were used for assessment of SHV size. However, in the presence of a contraindication to contrast, a non-contrast CT study may be used to fit a region of interest to the center of the radiopaque scaffold for measurement of SHV size.

CT image analysis. CT images were analyzed using commercially available post-processing software iNtuition (TeraRecon, Foster City, CA). Observers were blinded to the manufacturers' labeled SHV size. Analysis was performed as follows: First, the reconstruction phase with the best image quality, i.e. the least motion artifacts and sharpest basal ring contours were identified. Using multiplane reformats, a plane transecting through the basal ring was created by manipulating the cross-hairs in the corresponding views. For non-planar basal rings, a plane demonstrating a most complete basal ring was identified. Window levels were adjusted to a standard bone window, defined by a window level of 800HU and a width of 2000HU, for measurement with reduced metal blooming. Measurements were performed by fitting a circular region of interest to the center of the radiopaque scaffold, i.e. centered between the inner and outer contour of the radiopaque scaffold. The circular region yielded area in [mm²] and diameter [mm]. Measurements were performed three times with subsequent averaging of values in order to mitigate measurement error.

Statistical analysis. All continuous variables are expressed as mean \pm SD. Variables with non-normal distributions are presented as median with range. Pearson's correlations were used to test association between CT measurements and manufacturer labeled SHV size. Intra-class correlation was performed to determine inter-observer variability, and Bland-Altman analyses for comparison of CT SHV size measurement between two clinician observers. Statistical analysis was performed using Prism 7.

Supplement – Results

Across all valve sizes, the mean difference between the manufacturers' labeled SHV size and the CT assessed diameter of the circular ROI was -0.3 ± 0.2 mm for Perimount magna ease, -0.2 ± 0.2 mm for Perimount magna, -0.3 ± 0.2 mm for Perimount, -0.2 ± 0.2 mm for Mosaic, -0.5 ± 0.1 mm for Trifecta, 0.5 ± 0.1 mm for Mitroflow, 0.1 ± 0.1 mm for CE SAV, -0.2 ± 0.3 mm for Epic -0.4 ± 0.4 mm for Perimount 2700, and 0 ± 0.2 mm for Hancock.

Two CT imaging clinicians independently performed CT measurements for a subgroup of 75 SHVs, yielding an intraclass correlation coefficient of 0.99, indicating good inter-observer variability. Bland-Altman analysis showed good agreement between clinicians (Supplementary Figure 3).

Supplement – Discussion

For measurements, we deliberately assessed CT dimensions along the center of the visualized, radiopaque basal frame, in order to reduce the impact of acquisition and reconstruction technique as well as artifacts. CT-based assessment of SHV dimension can be affected by artifacts caused by the radiopaque component of the basal frame and sewing ring of stented SHVs. These artifacts include, blooming artifacts due to partial volume averaging as well as beam-hardening and streak artifacts.

In CT imaging of SHVs, the extent of blooming and streak artifacts are influenced by the following (7): 1) tube potential, with less artifact and less blooming at higher tube voltage; 2) reconstruction technique, with less artifacts with higher degree of iterative reconstruction or use of a monoenergetic image at higher energy levels; 3) reconstruction kernel, with less artifact when using a harder kernel, i.e. a stent kernel, compared to a standard soft tissue convolution kernel; 4) window setting at time of image assessment, with less depiction of artifact when using a large width window, such as a 'bone' window. Given these factors influence the appearance of the metal components, assessment of an internal diameter appears less robust. Instead, the technique employed in this study, namely purposefully measuring along the center of the visualized radiopaque basal frame, allows for relative independence from the above listed factors.

Supplementary Figure Legend

Supplementary Figure 1

Graphs of CT derived SHV size versus manufacturer labeled SHV, for **(a)** Perimount Magna Ease (Model 3300TFX) (Edwards Lifesciences), **(b)** Perimount Magna (Model 3000TFX) (Edwards Lifesciences), **(c)** Perimount (Model 2900) (Edwards Lifesciences), **(d)** Carpentier Edwards (CE) standard supra-annular valve (SAV) (Edwards Lifesciences),

Supplementary Figure 2

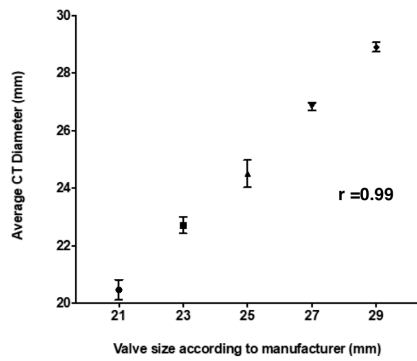
(Supplementary Figure 1 continued as Supplementary Figure 3) **(e)** Perimount (Model 2700) (Edwards Lifesciences) , **(f)** Mosaic (Model 305) (Medtronic), **(g)** Mitroflow (Sorin), **(h)** Trifecta (St. Jude Medical), **(i)** Epic (St. Jude Medical), **(j)** Hancock (Medtronic). Data are presented as mean \pm SD CT: Computed Tomography. Pearson's correlation coefficient (r) is presented for each graph.

Supplementary Figure 3

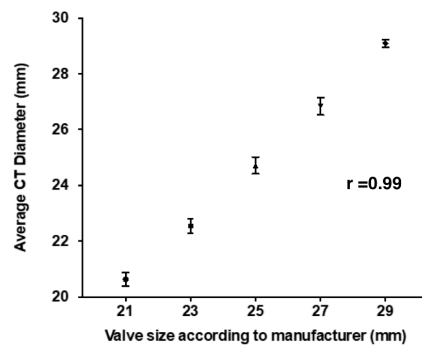
Bland-Altman Plot of CT based measurement of SHV size (diameter) for 2 clinician observers in a subgroup of the study cohort (n=75)

Supplementary Figure 1 – Graphs of measurements stratified by valve type and size

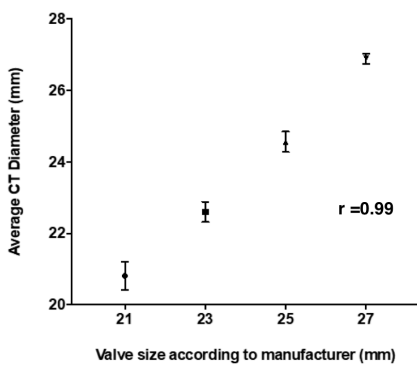
a Perimount Magna Ease (Model 3300TFX)



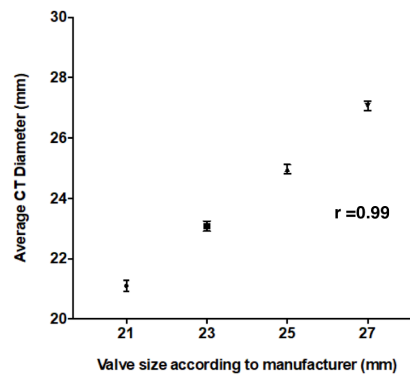
b Perimount Magna (Model 3000TFX)



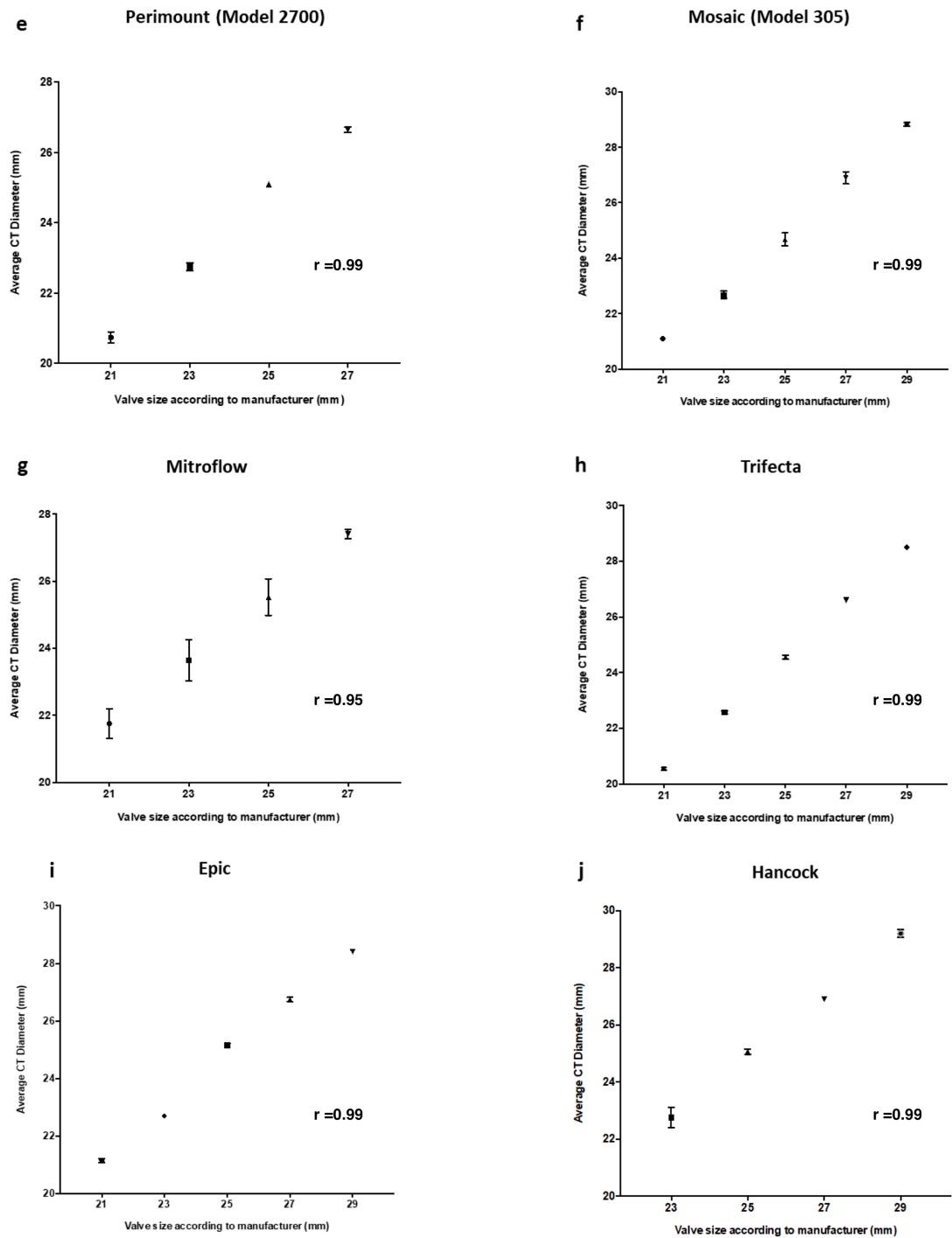
c Perimount (Model 2900)



d Carpentier-Edwards Supra-Annular valve (SAV)

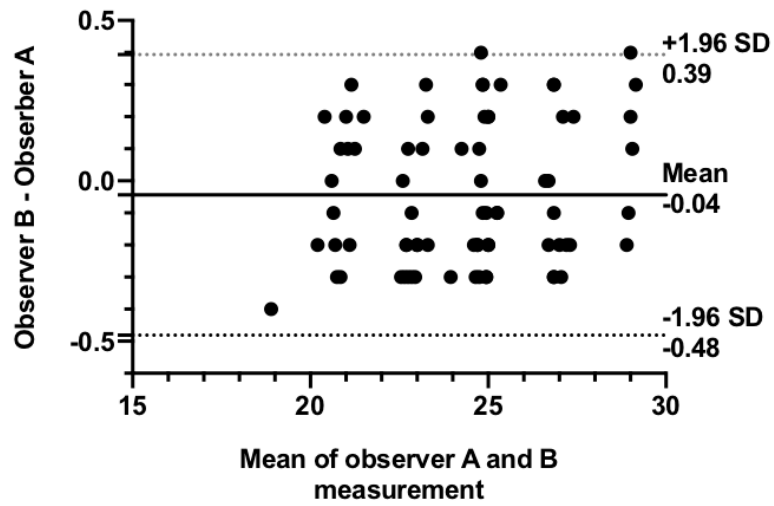


Supplementary Figure 2



Disclaimer : As a public service to our readership, this article -- peer reviewed by the Editors of EuroIntervention - has been published immediately upon acceptance as it was received. The content of this article is the sole responsibility of the authors, and not that of the journal

Supplementary Figure 3



Copyright EuroIntervention